Materials Transactions, Vol. 44, No. 2 (2003) pp. 247 to 252

Influence of the Matrix Microstructure on the Wear Resistance of Alumina Continuous Fiber Reinforced Aluminum Alloy Composites

Hirofumi Miyahara[1], Zou Xinguo[1,*1] Takashi Moriguchi[1,*2] and Keisaku Ogi[1]

[1]*Dept. of Materials Science and Engineering, Graduate School of Engineering, Kyushu University, Fukuoka 812-8581, Japan*

The solidification microstructure and wear resistant properties were investigated for alumina fiber reinforced Al alloy matrix composites. Alumina continuous fiber of 15 μm diameter was chosen to improve the wear resistance and clarify the wear mechanism. Al–7 to 27 mass%Si alloys, in which the hard Si phase was dispersed in matrix, and Al–4.5 mass%Cu, in which matrix showed age-hardening during heat treatment were used to evaluate the influence of hardness of matrix on wear resistant. Fiber reinforced composites were fabricated via the pressure infiltration process; continuous alumina fibers were placed in a graphite mold, then molten aluminum alloy was infiltrated into the fiber preforms in a vacuum to fabricate the composites specimens with the 55 vol% fiber. The pin on ring type wear resistance test was carried out under the condition of dry and air atmosphere. Wear resistant properties of fiber reinforced composites are improved about 2 to 10 times more than unreinforced alloys. Furthermore, Al–27 mass%Si hypereutectic alloy matrix composites, in which the hard primary Si particles are dispersed in eutectic matrix, shows higher wear resistance than that of hypoeutectic alloy, which consisted of primary dendritic α phase and α + Si eutectic structure. The primary Si hard phase in matrix connects the alumina continuous fibers and prevents the breakaway of fibers from the worn surface. The wear resistances are also increased by the age hardening of matrix for Al–4.5 mass%Cu and Al–7 mass%Si based alloy matrix composites.

(Received September 17, 2002; Accepted December 27, 2002)

Keywords: *solidification, alumina, continuous fiber, aluminum alloy, composites, dry sliding, wear resistance*

1. Introduction

Aluminum alloy matrix composites offer the potential for the high specific strength and stiffness in many applications. In terms of energy conservation and environmental protection, weight saving of parts is necessary in the transport such as, aircraft, automobiles and railway vehicles. Recent advances in the processing technology of aluminum alloy matrix composites have provided the high specific strength materials with improved friction and wear resistance for the application of commercial use such as brake discs and drams, engine pistons, cylinder liners, connecting rods, *etc.* In order to improve the wear resistance of composites, the principal tribological parameters that control wear performance of alumina fiber reinforced aluminum alloy composites are researched in two categories; mechanical and physical factor and materials factor.[1)] However, because of the complicity of the tribological phenomena, study of the influence of other parameters would be necessary for the application of commercial use of composite materials.

Axen *et al.*[2,3)] and Wang[4)] pointed out the importance of hardness of matrix alloy. It is necessary to focus upon micro-hardness of reinforcement and matrix phase and macro-hardness of composites. And besides hardness of matrix phase can change during wear resistance test due to the frictional heat. Moustafa and Jiang *et al.* suggested the influence of temperature on matrix microstructure during sliding tests.[5,6)] Perrin *et al.* also reported the continuous recrystallization in alumina short fiber reinforced Al–4.3 mass%Cu alloy composites.[7)] The heat from friction could cause the over-aging microstructure and reduce the matrix hardness and consequently cause a low wear resistance.

In this study, the dependence of hardness of matrix on the wear behavior was investigated in alumina fiber reinforced Al–Cu and Al–Si alloys composites. The continuous fibers, which aligned perpendicular to test surface in the cross-sections, were used in order to clarify the influence of fiber and microstructure of matrix on wear mechanism. A series of Al–Si hypo- and hypereutectic alloys were used to examine the influence of Si hard phase dispersed in a matrix on the wear resistance. Influence of age-hardening of α phase was also examined by using Al–Cu and Al–Si–Cu–Mg alloy matrix composites.

2. Experimental Procedure

A series of matrix alloys were prepared from 99.99 mass%Al (abbreviate to %), 99.9%Cu, 99.999%Si, and 99.97%Mg ingots, and then cast it into permanent molds as shown in Table 1. Al–7%Si and Al–4.5%Cu alloys are used as standard in this study. Al–12, 18, and 27%Si alloys were used to examine the influence of Si hard phase dispersed in a matrix on the wear resistance. The age-hardenable elements such as Mg and Cu were added in order to evaluate the influence of hardness of α phase. An alumina continuous

Table 1 Chemical compositions of specimens (mass%).

Materials	Si	Cu	Mg	Al
Al–7Si	7.24	—	—	Balance
Al–4.5Cu	—	4.43	—	
Al–12Si	12.85	—	—	
Al–18Si	17.41	—	—	
Al–27Si	26.80	—	—	
Al–4.5Cu–1.6Mg (T6 treatment)	—	4.38	1.65	
Al–7Si–3Cu–0.4Mg (T6 treatment)	7.15	2.80	0.43	

*1Graduate Student, Kyushu University.
*2Graduate Student, Kyushu University. Present address: Toray Industries, Inc., Tokyo 103-8666, Japan.

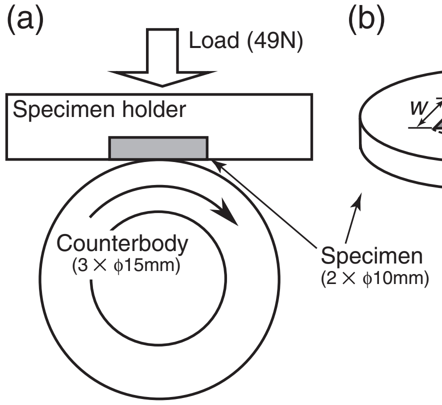

Fig. 1 Schematic illustration of specimen and counterbody of dry sliding test.

fiber (ALTEX, Sumitomo Chemical Co., Ltd., 15 µm diameter, γ-Al_2O_3) was used for reinforcement. A pressure infiltration apparatus, consisting of a vacuum chamber and an electric furnace that included a cylinder, a mold, and a piston made of graphite, was used to fabricate the composites and unreinfrced alloys.[8)] A preform made of loose alumina continuous fibers was fit tightly into the mold, and a block of matrix alloy was placed above the mold. The matrix alloys melted in a cylinder were infiltrated at 1073 K into the alumina preform at a pressure of 14 MPa and solidified along fibers from bottom to top at a rate of 500 µm/s to form the 10 mm diameter and 40 mm long composite ingots in a vacuum atmosphere of 2–3 Pa. The volume fraction of fibers was found to be approximately 55%.

The composites and unreinforced specimens were sliced into 2 mm-thick disks for dry sliding test. The specimen was fixed in a specimen holder of a block-on-ring type dry sliding machine (OAT-U, Tokyo Testing machine MFG Co., Ltd.) as shown in Fig. 1. As shown in the previous paper, the wear behavior of composites depends on the fiber alignment.[9)] The sliding surface of each specimen was prepared to be perpendicular to the fiber allay, since this allay gives a better and consistent wear resistance. Age hardenable specimens were performed solution heat-treatment at 773 K for 10 hours followed by quenching in an ice water and aging at 433 K for duration of 10^3 min in a silicon oil bath. The 30 mm diameter and 3 mm thick JIS-SUJ2 bearing steel, which has quenched and tempered to reach HRC63 hardness, was used as a counterbody. The test was carried out at a constant normal load of 49N, a constant sliding velocity of 0.94 m/s and sliding distance from 100 to 1800 m at a room temperature. A wear resistance was evaluated by measuring the volume loss (ΔV) due to the wear at each wear distance using following equation.

$$\Delta V = w\left\{r^2 \sin^{-1}\left(\frac{b}{2r}\right) - \frac{b}{2}\sqrt{\left(r^2 - \frac{b^2}{4}\right)}\right\} \tag{1}$$

where w (3 mm) is the width and r (15 mm) is the radius of sliding ring, and b is the length of worn surface. The worn surface and the cross-section of the specimen were analyzed by an optical microscope (OM), secondary electron microscopy (SEM), X-ray diffraction (XRD) and electron probe micro analyzer (EPMA).

3. Results and Discussion

3.1 Influence of hard phase in matrix alloy on wear resistance

The microstructures of the unreinforced matrix alloy and composites specimens for Al–Si alloy system are shown in Fig. 2. Primary α dendrite and eutectic structure between dendrites are observed in as-cast Al–7%Si hypoeutectic matrix alloy (figure (a)). The dendrite, however, becomes a little finer and eutectic phase forms around the distributed fibers (figure (b)), since the distributed fibers reduce the diffusion layer of primary α phase and give a thermal, solutal and geometrical influence on the solidification of matrix alloy.[10,11)] In Al–12%Si alloy system, eutectic structure matrix is composed both in unreinforced alloy and composites (figures (c, d)). Large primary Si phase grows when the Si content exceeds the eutectic composition, and the volume fraction of primary Si phase becomes larger with increasing the Si content (figure (e)). In composites specimen, the size of primary Si reduces a little because of the presence of alumina fibers as same as a primary α phase in hypoeutectic structure (figure (f)). However, the primary Si growth is barely influenced by fiber distribution. Consequently, Si phase touches to the alumina continuous fibers and the hard phases (alumina+Si) support each other and become the network type distribution against the sliding surface.

Figure 3 shows the relationship between wear volume loss and sliding distance for the alumina/Al–Si alloy composites. The results on unreinforced matrix alloys were also drawn in this figure. In Al–7%Si hypoeutectic matrix alloy, the volume loss reaches 0.8 mm^3 only at 100 m of sliding distance. The volume loss of hypereutectic matrix alloy, however, decreases to 0.2 mm^3. Primary Si significantly improves the wear

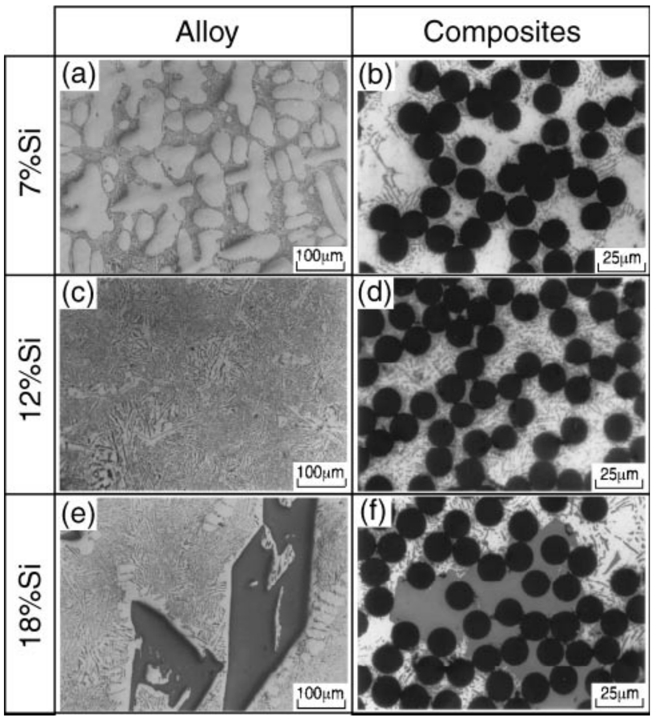

Fig. 2 Micrographs on transversal section for Al–Si alloys (a, c, e) and alumina/Al–Si composites (b, d, f).

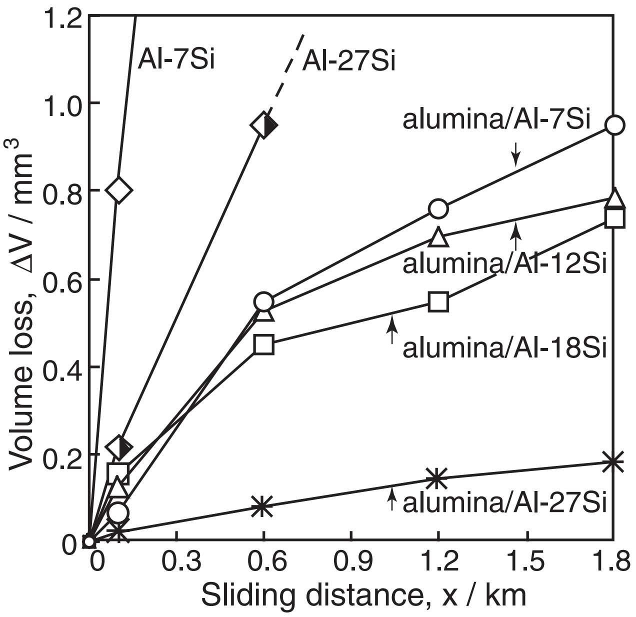

Fig. 3 Relationship between volume loss and sliding distance for Al–Si alloys and alumina/Al–Si composites.

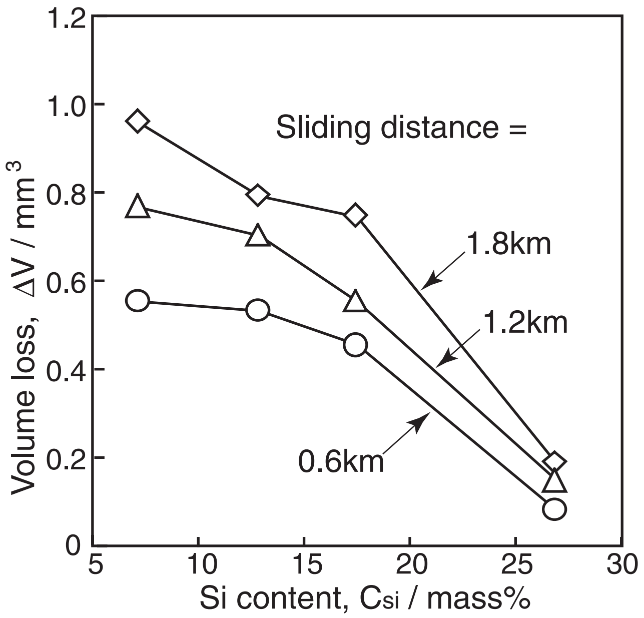

Fig. 4 Relationship between volume loss and Si content for Al–Si alloys and alumina/Al–Si composites.

resistance of unreinforced alloys. The volume loss is lowered by the reinforcement of alumina fibers. Although the specimen is rapidly worn until 600 m, wear speed gradually decreases as the composites specimen slides longer. This rapid wear at the initial stage can be ascribed to the initial wear period caused by the small contact area by a microscopic rough surface or the high applied compressive stress by the pinpoint contact of the counterbody. As shown in Fig. 3, the volume losses of Al–18 and 27%Si hypereutectic composite are lower than hypoeutectic and eutectic composite specimens. This could be attributable to the presence of primary Si which forms the network type distribution of hard phase. Hence, the relationship between Si content and the volume loss were summarized in Fig. 4. As the Si content and the volume fraction of primary Si phase increases, the volume loss decreases. Especially, Al–27%Si matrix composites extremely decreases the volume loss. To reveal the influence of hard phases, the macroscopic and microscopic analyses were made on the transverse cross-sections parallel to the sliding surfaces of unreinforced alloys and composites as shown in Figs. 5 and 6, respectively. In the case of unreinforced alloys, the plastic deformation flow of dendrites is clearly observed near the worn surface in Al–7%Si matrix alloy as shown in Fig. 5(a) and Fig. 6(A). About 80 μm thickness of layer, which consist of the mixture of debris of the counterbody, the specimen and oxides, was observed in the vicinity of worn surface. The lump of debris can scratch the matrix deeply and act as abrasive in three-body-type abrasion. On the contrary, in Al–27%Si matrix alloy, this debris-layer barely observed on the worn surface and the deformation of eutectic matrix decreases (Fig. 5(b), Fig. 6(B)). In stead of less deformation layer, many microcracks was observed in the primary Si phases distributed near worn surface. Si hard phase could restrain the strain and delamination of eutectic structure near the worn surface. In the composites, the matrix is less deformed due to the existence of alumina fibers even in the hypoeutectic matrix

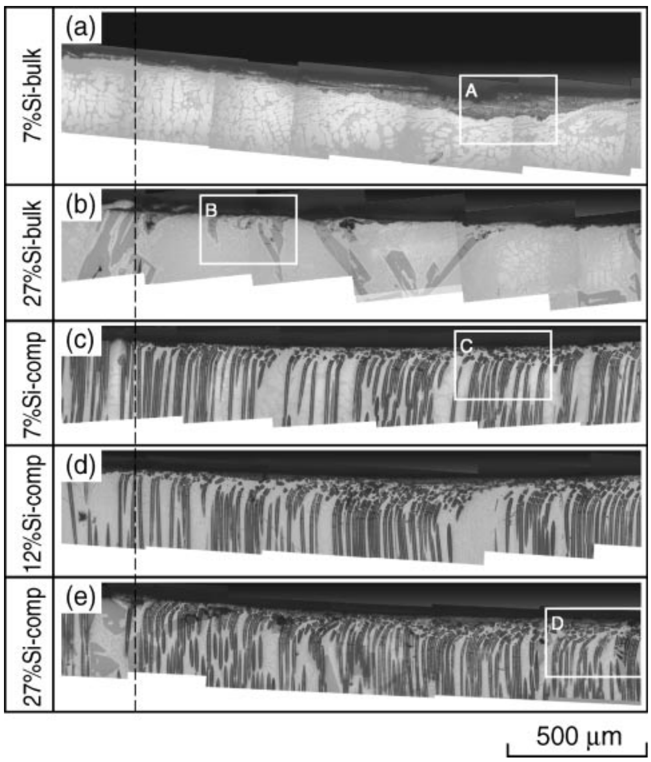

Fig. 5 Macroscopic view on transversal section for Al–Si alloys (a, b) and alumina reinforced alloys (c–e). Rectangular area of A–D is magnified and shown in Fig. 6.

alloy as shown in Fig. 5(c) and Fig. 6(C). However, matrix alloy deforms and continuous fibers are tilt a few degrees from the perpendicular line. From the microscope observation, the worn surfaces of the counterbody and the specimen are scratched each other and many debris are located on the worn surface. EPMA and XRD analysis revealed that debris consist of Al, Fe, Al_2O_3 and Fe_2O_3. Therefore, the metals exfoliate from the surfaces of both of the specimen and the

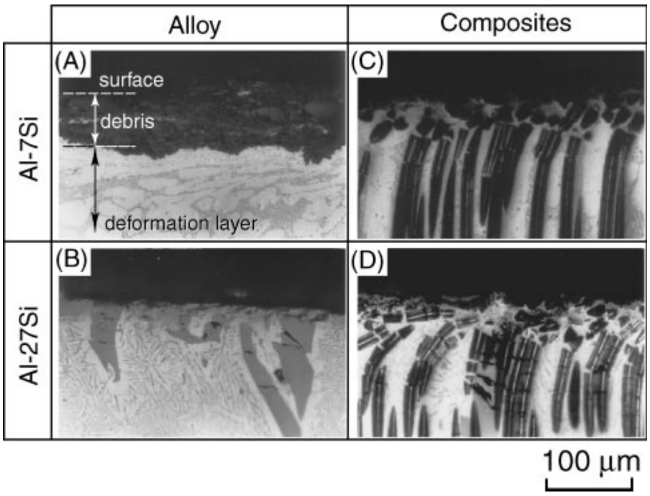

Fig. 6 Micrographs on transversal sectin for Al–Si alloys (A,C) and alumina reinforced Al–Si alloys (B,D) in Fig. 5.

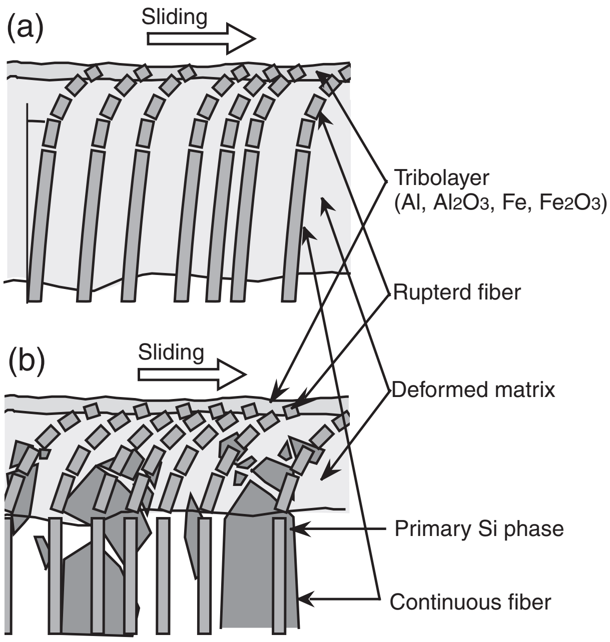

Fig. 7 Schematic illustration of wear behavior for Al–Si hypoeutectic alloys matrix composites (a) and hypereutectic alloys composites (b).

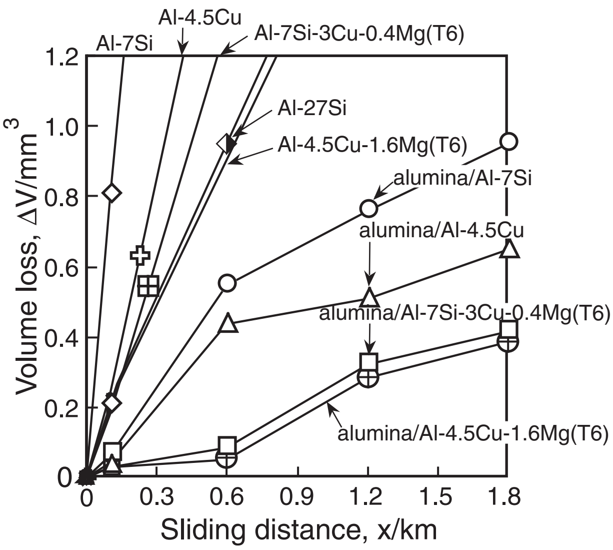

Fig. 8 Influence of age hardening on dry sliding for Al–Si and Al–Cu alloy composites and unreinforced alloys.

counterbody, and oxidized during test to become Al_2O_3 and Fe_2O_3 debris in the vicinity of the worn surface. Some broken alumina fiber can be directly mixed with debris, since the chips of alumina fibers are appeared on the mechanical mixed layer of the surface. Below the sliding surface, continuous fibers gradually draw a curve from the initial array to the worn surface. These shear strain layer was reported by Moustafa[5)] and Jiang and Tan[6)] in alumina short fiber reinforced Al–Si alloy composites and Venkataraman and Sundararajan[12)] in SiC particle reinforced Al composites. This shear strain flow beneath the worn surface was clearly observed in present work, since continuous fibers were perpendicular to the sliding surface as an indicator before wear tests. Most of models of wear mechanism for composites were establish at particle or short fiber at low fiber-volume fraction from 5 to 30%. However, continuous fiber clearly indicates the influence of matrix hardness on wear phenomena. That is, the reinforcement bend a few degrees inside of the specimen and broken near the worn surface in the soft matrix such as hypoeutectic structure as shown in Fig. 7(a). When the hard hypereutectic alloy is used for matrix, both of Si hard phase and alumina fiber prevent both of the plastic deformation of matrix and the breakaway of fibers from the worn surface (Fig. 7(b)).

3.2 Influence of matrix microstructure and hardness on wear resistance

The influence of wear test condition on the wear volume loss was generally described as,

$$W = k\frac{P \cdot S}{H_v} \tag{2}$$

where W is the wear volume, P the applied load, S sliding distance, H_v the Vickers hardness of matrix alloy or composites, and k the wear coefficient.[13)] Since the Vickers hardness can be a predominant variable parameter when the specimen slides same sliding distance, the influence of increasing of the hardness of matrix by age hardening on wear resistance characteristics is investigated for the alumina/Al–Cu, Al–Si based alloy matrix composites as shown in Fig. 8. In un-thermal treated Al–4.5%Cu alloy, the volume loss is reached about 1 mm^3 at 300 m of sliding distance. However, in peak-aged Al–4.5%Cu–1.6%Mg alloy, the volume losses are almost 60% of that in Al–4.5%Cu alloy, while the microstructure is the mixture of primary α phase and eutectic structure. The age hardening increases the micro hardness of α phase (Table 2(b)) and the macro hardness about three times (Table 2(a)). The enhancement of hardness, eventually increases the wear resistance. The wear resistance of T6-thermal treated Al–7%Si–3%Cu–0.4%Mg alloy is also superior to that of Al–7%Si alloy. And besides, the macro-hardness of Al–27Si alloy is higher as shown in Table 2(a), that indicates the dispersion of Si hard phase can also raise both of macrohardness and wear resistance. In the same way, the increasing of hardness of matrix via age hardening

Table 2 Macro and micro Vickers hardness of alloys and composites. (a) macro Vickers (load = alloys: 10 kg, composites: 20 kg). (b) micro Vickers (load = 25 g).

(a) macro Vickers (load = alloys: 10 kg, composites: 20 kg).		
Materials	Alloys	Composites
Al–4.5Cu	57.0	163.8
Al–4.5Cu–1.6Mg (T6)	150.7	282.4
Al–7Si	47.2	107.8
Al–7Si–3Cu–0.4Mg (T6)	117.0	240.9
Al–12Si	54.6	120.8
Al–27Si	66.2	163.5

(b) micro Vickers (load = 25 g).		
Phase	Materials	Alloys
primary α	Al–4.5Cu	63
primary α	Al–4.5Cu–1.6Mg (T6)	142.3
primary α	Al–7Si	46.9
primary α	Al–7Si–3Cu–0.4Mg (T6)	131.7
primary Si	Al–18Si	829.1
alumina	alumina fiber	1800–1900

process and *in-situ* Si phase dispersion reduces the wear loss in aluminum alloy matrix composites; the volume loss of Al–7%Si–0.4%Mg alloy and Al–4.5%Cu–1.6%Mg alloy matrix composites become smaller than Al–7%Si and Al–4.5%Cu alloy matrix composites in whole sliding distance. Although the hardness of alumina fiber is as ten to twenty times high as those of matrix, the wear resistance is drastically influenced by the micro- and macrohardness of matrix alloys. Incidentally, the volume loss of these age-hardenable matrix composites increases over 1.2 km of sliding distance. This sudden change can be attributed the over precipitation and softening of matrix by the frictional heat, but more detailed studies are necessary to conclude the thermal influence during the wear test.

Since the wear resistance can be related with the macro hardness, specific wear rate, which are defined as the wear rate per unit load and unit sliding distance, are summarized in relation with macro hardness in Fig. 9. Figure 9(b) is magnified copy of dark area in Fig. 9(a). In Al–Si system, Al–7%Si alloy has softest matrix and highest specific wear rate in the present work as shown in Fig. 9(a). However, the wear rate or Al–7%Si alloy reduces with increasing hardness by (i) fabrication with alumina continuous fiber, (ii) increasing the Si content and dispersion of Si hard phase, and (iii) addition of the age hardenable elements and heat treatment. The wear rate of Al–Cu alloy system is also decreased with fabrication with alumina fibers or age hardening, as shown in figure (a) and in composites in figure (b). Furthermore, the slope of line connected from Al–7Si alloy to Al–27Si alloy leans more than that to Al–7Si–3Cu alloy, which indicates that the effect of the mixing hard phase is more significant than that of age hardening to improve the wear resistance.

4. Summary

The solidification microstructure and wear resistant properties were investigated for alumina fiber reinforced Al–Si and Al–Cu based matrix alloy composites. The results

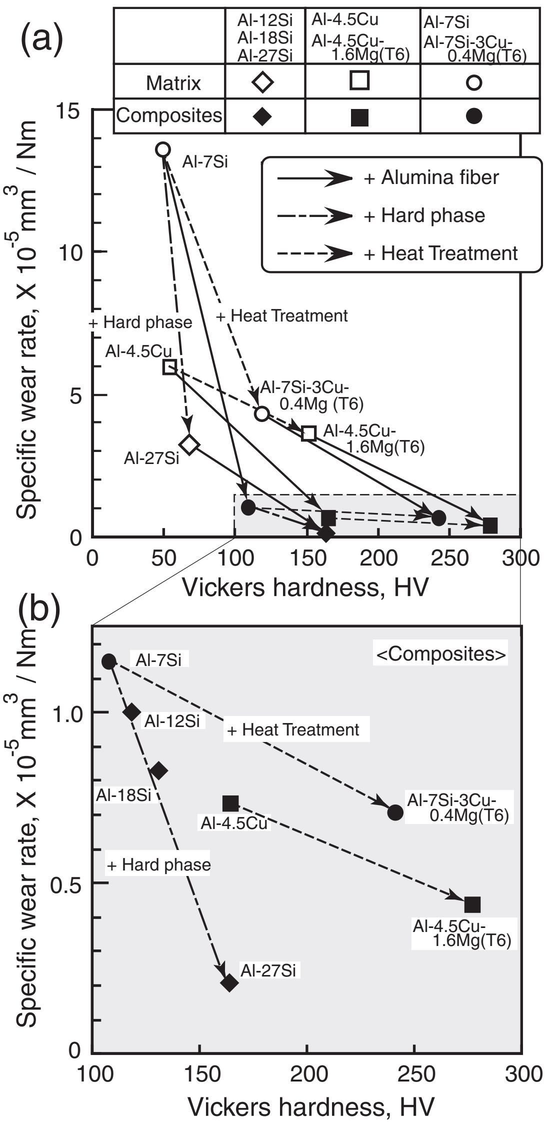

Fig. 9 Relationship between micro vickers hardness and specific wear rate for unreinforced alloy and composites. Figure (b) is an enlarged copy of area surrounded by broken line in figure (a).

obtained are summarized as follows:

(1) Wear resistant properties of fiber reinforced composites were improved about 2 to 10 times more than unreinforced alloys. Alumina fibers were, however, broken and drifted along the worn surface.
(2) The hypereutectic matrix alloy of Al–27 mass%Si, in which the Si hard particles were dispersed in matrix, showed higher wear resistant than Al–7 mass%Si alloy, which consisted in only α phase and small amount of eutectic structure. The hard phase in matrix could connect the alumina continuous fibers, and prevent the breakaway of fibers from the worn surface.
(3) The wear resistance was also improved by the age hardening of matrix for both of Al–Cu and Al–Si based alloys and these alloys matrix composites. The increasing of hardness of α phase could increase the wear resistance.

REFERENCES

1) A. P. Sannino and H. J. Rack: Wear **189** (1995) 1–19.
2) N. Axen and S. Jacobson: Wear **178** (1994) 1–7.
3) N. Axen, A. Alahelisten and S. Jacobson: Wear **173** (1994) 95–104.
4) I. M. Hutchings and A. G. Wang: Philos. Mag. A **57** (1988) 197–206.
5) S. F. Moustafa: Wear **185** (1995) 189–195.
6) J.-Q. Jiang and R.-S. Tan: Wear **195** (1996) 106–111.
7) C. Perrin and W. M. Rainforth: Wear **181–183** (1995) 312–324.
8) H.-N. Liu, H. Miyahara and K. Ogi: Mater. Sci. Tech. **14** (1998) 292–298.
9) H.-N. Liu and K. Ogi: J. Mater. Sci. **34** (1999) 5593–5599.
10) H. Miyahara and K. Ogi: Mater. Trans., JIM **42** (2001) 252–257.
11) H. Miyahara and K. Ogi: Mater. Trans., JIM **42** (2001) 258–262.
12) B. Venkataraman and G. Sundararajan: Acta Mater. **44** (1996) 461–473.
13) J. F. Archard: J. Appl. Phys. **24** (1953) 981–988.